1963

Effects of demagnetizing fields on the measurements of dispersions of magnetic anisotropy in thin ferromagnetic films

James Michael Daughton
Iowa State University

EFFECTS OF DEMAGNETIZING FIELDS ON THE MEASUREMENTS OF DISPERSIONS OF MAGNETIC ANISOTROPY IN THIN FERROMAGNETIC FILMS

by

James Michael Daughton

A Dissertation Submitted to the
Graduate Faculty in Partial Fulfillment of
The Requirements for the Degree of
DOCTOR OF PHILOSOPHY

Major Subject: Electrical Engineering

Approved:

Signature was redacted for privacy.

In Charge of Major Work

Signature was redacted for privacy.

Head of Major Department

Signature was redacted for privacy.

Dean of Graduate College

Iowa State University
Of Science and Technology
Ames, Iowa

1963

TABLE OF CONTENTS

		Page
I.	INTRODUCTION	1
II.	THEORY	15
	A. Demagnetizing Fields	15
	B. Magnetization Buckling	17
	C. Angular Dispersion	24
III.	EXPERIMENTAL DATA	33
IV.	DISCUSSION	45
V.	BIBLIOGRAPHY	47
VI.	ACKNOWLEDGEMENTS	48
VII.	APPENDIX	49
	A. Calculation of the Demagnetizing Field for Circular Films	49
	B. Graphical Solutions Using the Switching Asteroid	53
	C. Effect of Size on the Number of Domains in a Film	58

I. INTRODUCTION

Much work has been done recently on the dispersions or variations of the magnetic anisotropy in thin magnetic film materials (2,5,7,8). As background for a discussion of these dispersions, a brief discussion of the quasi-static behavior of thin magnetic films is presented.

A torque per unit volume $\underline{T}$ on the magnetization $\underline{M}$ due to an applied field $\underline{H}$ is found to be $\underline{M} \times \underline{H}$ from basic considerations (4). In thin magnetic films there is another torque which is a material property. This torque per unit volume tends to restore $\underline{M}$ to a rest or easy axis in the plane of the film with a strength of $MH_K \sin \theta \cos \theta$, where H_K is called the anisotropy field and θ is the angle of rotation of $\underline{M}$ from the easy axis. Along the easy axis are two easy directions. Perpendicular to the easy axis is the hard axis which corresponds to two hard directions. Figure 1a illustrates a film and associated applied fields. The magnitude of $\underline{T}$ tending to restore $\underline{M}$ to the easy axis is

$$T = M(h_L \sin \theta + H_K \sin \theta \cos \theta - h_T \cos \theta).$$

If $\underline{M}$ rotates to a position of zero torque, then

$$h_L \sin \theta + H_K \sin \theta \cos \theta - h_T \cos \theta = 0.$$

This equation may be interpreted as a relationship between the field components h_L and h_T with θ as a parameter. A family of straight lines results as illustrated in Figure 1b. The magnetization is not stable along all of each line. Points of marginal instability may be found by eliminating θ between the equations $T = 0$ and $\partial T/\partial \theta = 0$. The result is that

Figure 1. The directional M-H characteristics of a thin magnetic film and associated coordinate system.

a) The coordinate system.

b) The M-H characteristic in the easy direction.

c) The M-H characteristic in the hard direction.

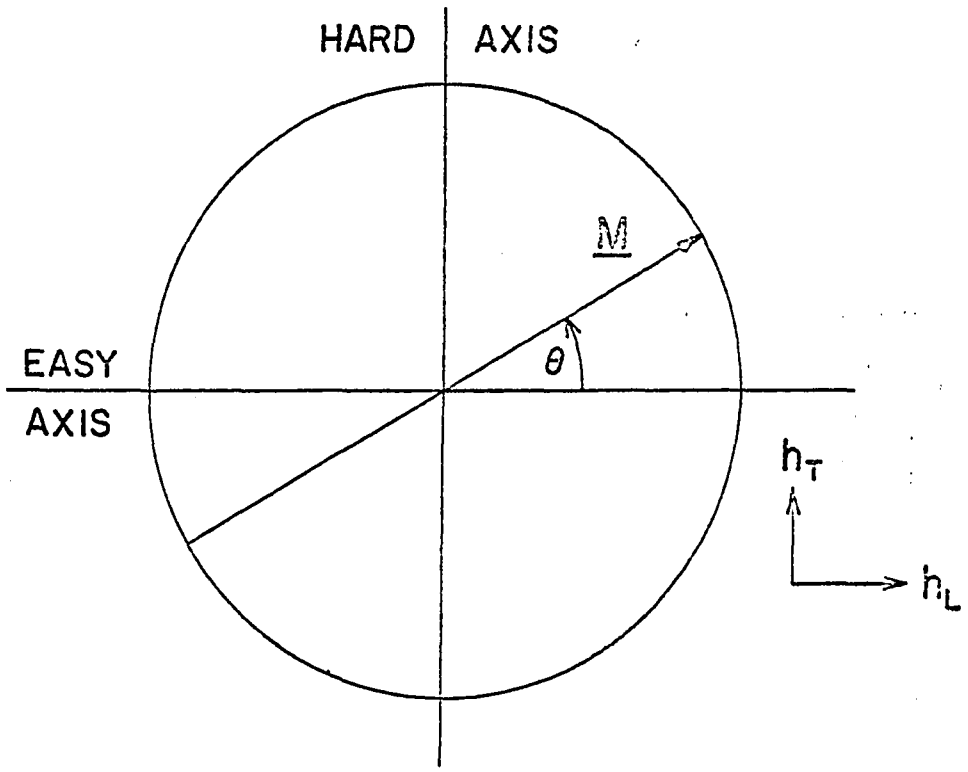

(a)

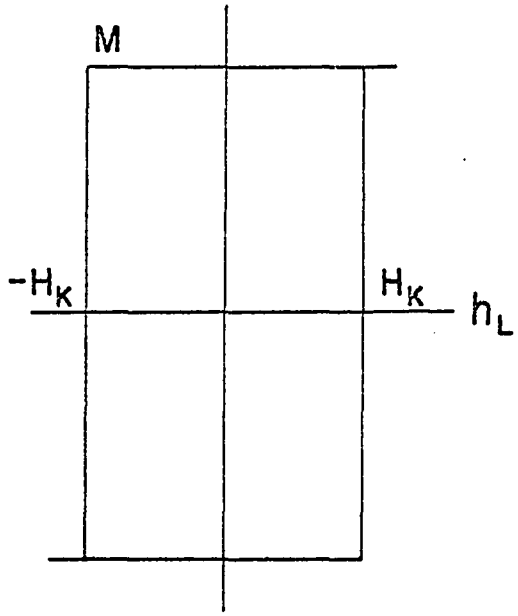

(b)

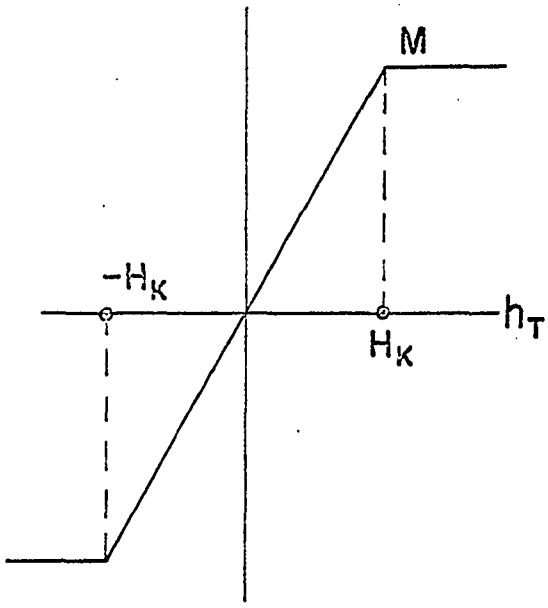

(c)

$$(h_L/H_K)^{2/3} + (h_T/H_K)^{2/3} = 1,$$

which is the asteroid illustrated in Figure 16. It may be seen that if $h_T = 0$, no torque is applied to $\underline{M}$ by h_L. However, if h_L exceeds H_K anti-parallel to $\underline{M}$, then $\underline{M}$ is unstable and must rotate 180 degrees. This behavior would suggest the easy-direction hysteresis loop in Figure 1b. If $h_L = 0$ it is found from the torque equation that $M \sin \theta = Mh_T/H_K$. Figure 1c illustrates the ideal behavior of the hard-direction component of $\underline{M}$ with an applied hard direction field. An experimental deviation from this ideal film behavior of the magnetization is observed in that instability of the magnetization does not appear to occur for the calculated combinations of h_L and h_T. To explain some of the deviations, it has been suggested that the effective easy axis of magnetization for a thin film is an average of dispersed easy axes throughout the film. This variation is commonly called the dispersion of the easy axis or the angular dispersion. In a like manner the variation of the anisotropy field H_k is called dispersion of H_k or the magnitude dispersion. Some dispersion of magnetic properties in a film certainly exists due to non-uniform stresses, chemical inhomogeneities, non-uniform deposition fields, thickness variations, angle of incidence effects, thermal agitation, and other possible causes. The purpose of this investigation is to demonstrate that demagnetizing effects can explain results which have been heretofor interpreted as being caused by dispersions of the magnetic properties.

The most common methods of measuring apparent angular dispersion use crossed-field techniques. Only the particular method used to make the

measurement for this thesis will be discussed in detail here. A sinusoidal field with an amplitude much larger than H_K is applied in the hard (transverse) direction while simultaneously a small and constant field is applied in the easy (longitudinal) direction. A typical dynamic behavior of the magnetization is illustrated in Figure 2. The top row of figures in Figure 2a represents typical hard-direction M-H curves for three different values of the longitudinal field h_L. As the longitudinal field is increased from zero, the loop tends to close. The bottom row in Figure 2a represents the easy-direction component of magnetization as a function of transverse field for the same three values of h_L used in the top row. With a zero longitudinal field very little net magnetization in the easy direction is observed because the film demagnetizes into many small domains such that the magnetization components along the easy axis average to zero. As the longitudinal field is increased, a net magnetization in the direction of the longitudinal field results. The maximum easy-direction component of magnetization Mp for a given h_L occurs at roughly the same value of h_T which gives a zero value of the transverse component of magnetization. For sufficiently large longitudinal fields the magnetization remains essentially a single domain. A further increase in longitudinal field no longer causes the maximum easy-direction magnetization to increase. Figure 2b schematically represents the distribution of the net magnetization during one cycle of transverse field. States are labeled with numbers which correspond to points on the M-H curves in Figure 2a. Figure 2b is not intended to indicate a domain structure.

The determination of apparent angular dispersion of a film from data

Figure 2. Dynamic behavior of magnetization during an angular dispersion measurement.

a) Easy- and hard-direction M-H loops.

b) States of average magnetization.

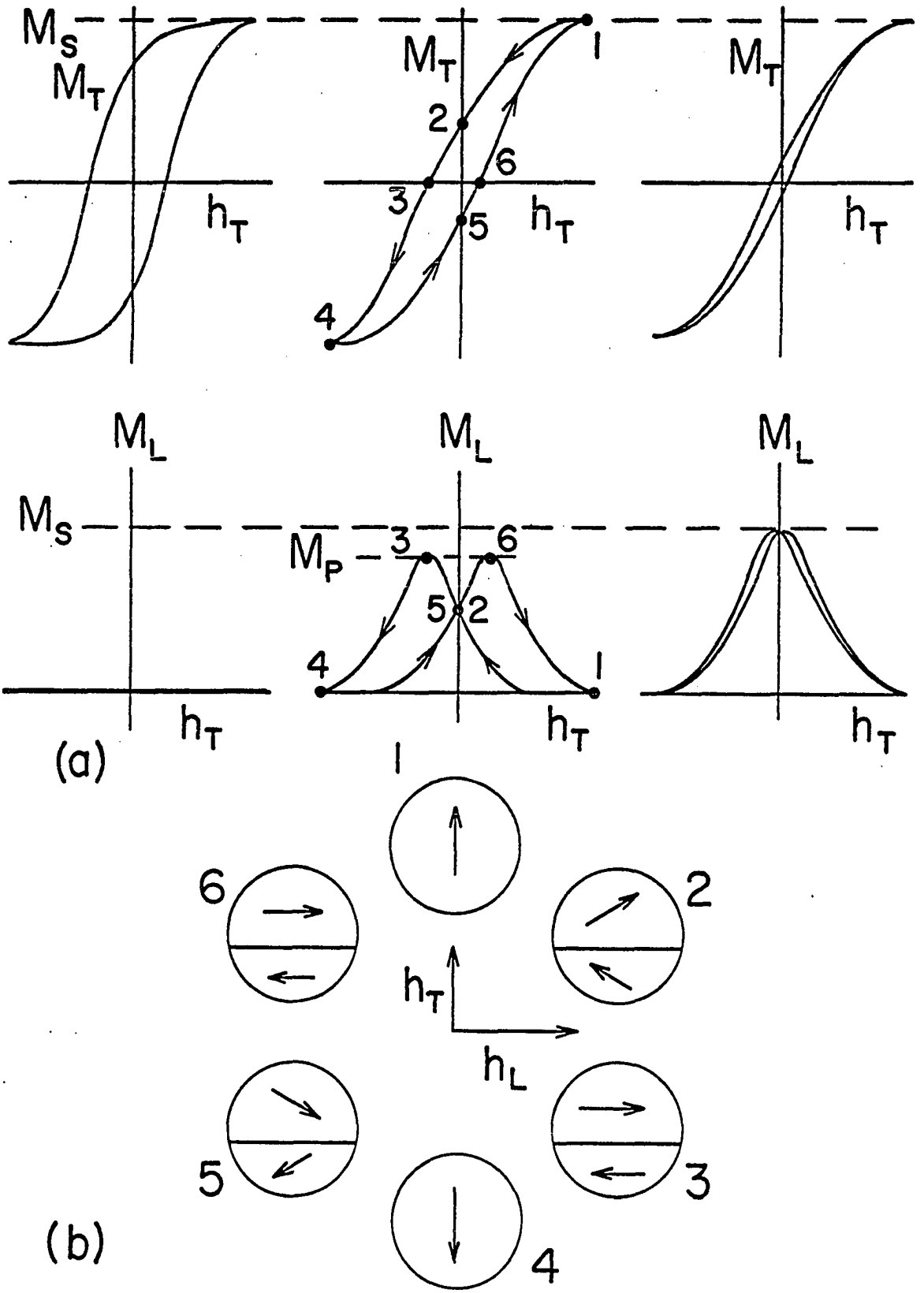
M_S
M_T
h_T
M_T
1
2
3
4
5
6
h_T
M_T
h_T
M_L
M_S
h_T
M_L
M_P
3
6
5
2
4
1
h_T
M_L
h_T
(a)
1
6
2
h_T
h_L
5
3
4
(b)

of the type described in the previous paragraph is made by assuming the film is divided into many non-interacting segments, each segment having its own easy direction. If the magnetization is rotated to an angle greater than 90° with respect to its initial easy axis, the magnetization is presumed to change its easy direction by 180°, or to "switch". Hence, a large alternating transverse field would cause half the film segments to be in one state and half in the other provided the distribution of easy axis about the average easy axis is symmetrical. If a constant field in the easy direction is also applied, some of the segments should switch to the direction of this field and a net magnetization in the direction of the applied field should result. Assuming this model to be correct, one would expect most of the magnetization to be in one state when the longitudinal field is sufficiently large to cause most of the regions with the largest deviations of easy directions to switch. If most of the dispersed easy directions make an angle less than α with the average easy direction, then a longitudinal field of $H_k \sin \alpha$ should cause most of the magnetization in the film to rotate as a single domain. Hence the so-called dispersion angle α would be given by $\sin^{-1} \frac{h_L}{H_k}$, or if α is small, by $\frac{h_L}{H_k}$.

Let ϵ designate the ratio of the peak magnetization in the easy direction for a given h_L to the saturation magnetization, i.e., let $\epsilon = M_p/M_s$ as interpreted in Figure 2a. Typical experimental results for ϵ as a function of h_L are shown in Figures 3 and 4. The data illustrated in Figure 3 were taken using films having approximately the same thickness and magnetic properties. Films No. 2 through No. 6 were all cut from film No. 1. The data illustrated in Figure 4 were taken on four 5/8 inch

Figure 3. Experimental behavior of ϵ as a function of h_L for some 2000A^{o} thick rectangular films with $H_K \simeq 3.2$oe. Film 1, 0.8" x 0.8". Film 2, 0.43" x 0.43". Film 3, 0.26" x 0.26". Film 4, 0.20" x 0.26". Film 5, 0.15" x 0.15". Film 6, 0.11" x 0.11".

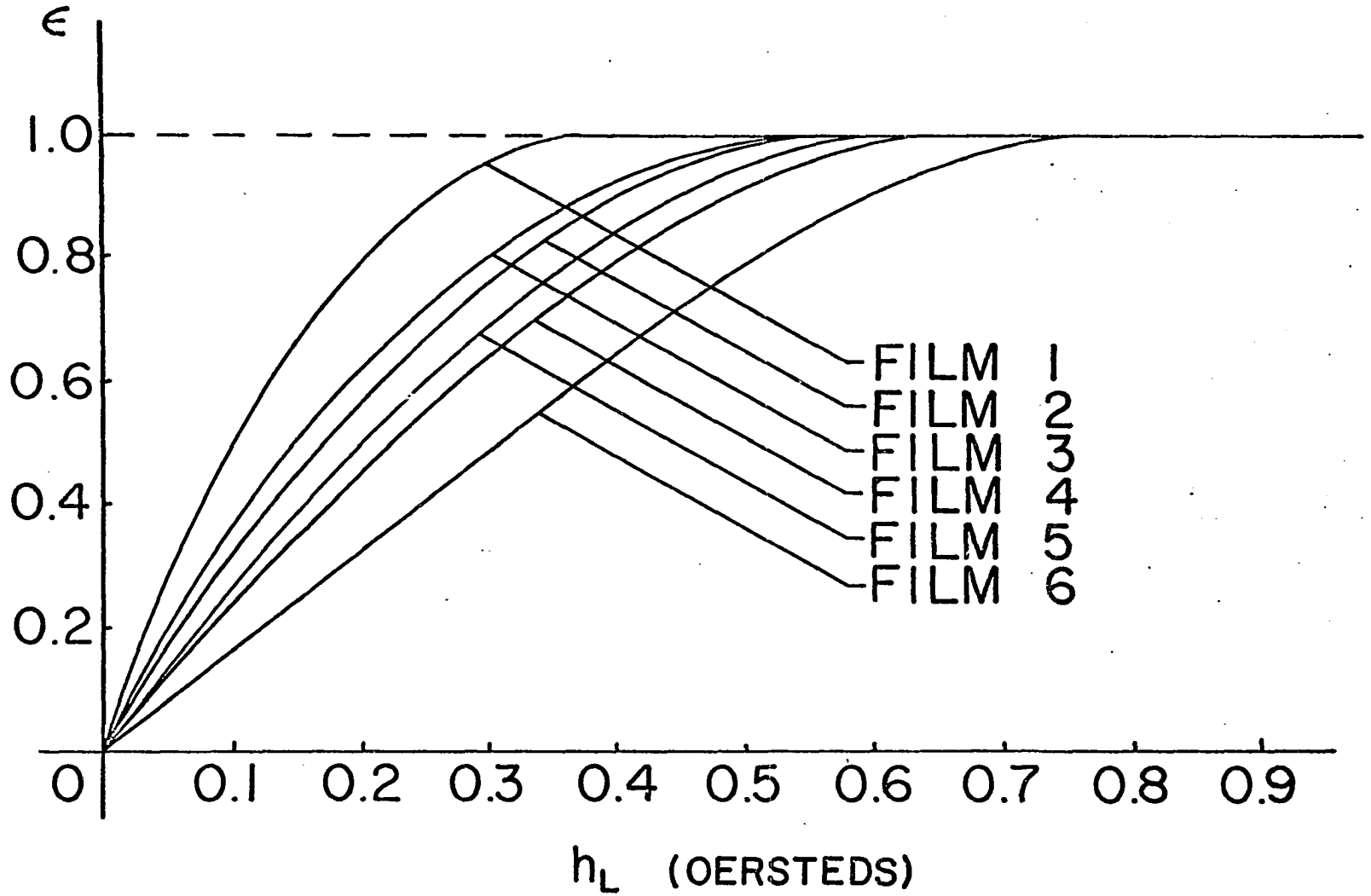
ϵ
1.0
0.8
0.6
0.4
0.2
0
0.1
0.2
0.3
0.4
0.5
0.6
0.7
0.8
0.9
FILM 1
FILM 2
FILM 3
FILM 4
FILM 5
FILM 6
h_L (OERSTEDS)

Figure 4. Experimental behavior of ϵ as a function of h_L for some 5/8" diameter circular films with $H_K \simeq 2.4$oe. Film 1, 1100A°, Film 2, 1600A°, Film 3, 1800A°, Film 4, 1950A°.

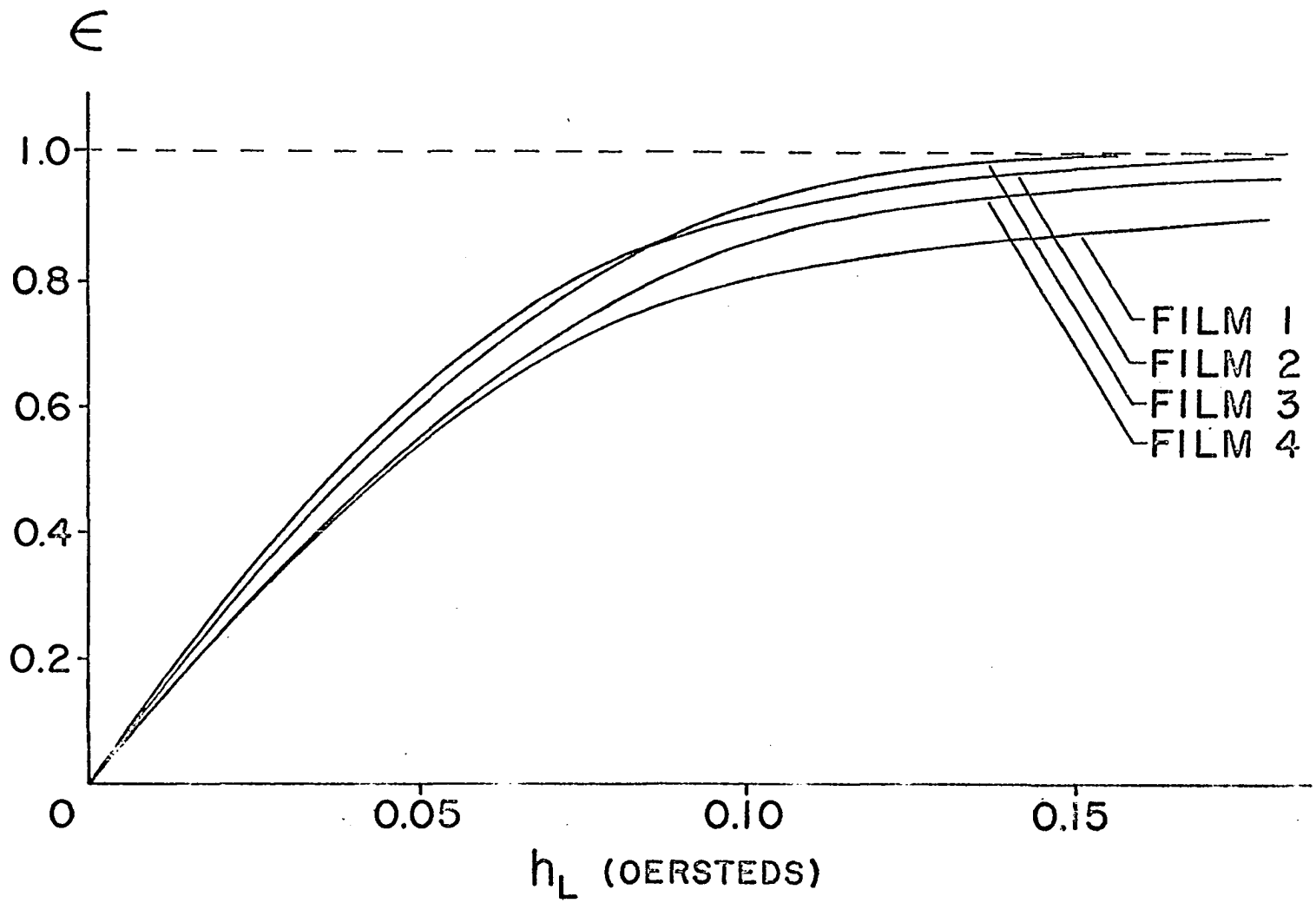
ϵ
1.0
0.8
0.6
0.4
0.2
0
0.05
0.10
0.15
h_L (OERSTEDS)
FILM 1
FILM 2
FILM 3
FILM 4

diameter circular films of different thicknesses. It is seen that ϵ approaches unity asymptotically. Hence the value of h_L necessary to produce saturation is not usually taken as the measure of dispersion, but rather the value of h_L which gives an ϵ of 0.83 or some other similar fraction. If an ϵ of 0.83 is selected, then the values of $\sin^{-1} h_L/H_k$ at $\epsilon = 0.83$ range from less than 2^o to more than 10^o for the data illustrated in Figures 3 and 4.

There are many schemes for measuring apparent dispersion of the easy axis which are very similar to the crossed-field method described here. Some use pulses rather than alternating transverse fields. Others use the magnitude of the time derivative of longitudinal magnetization instead of the longitudinal magnetization to determine ϵ. The latter method gives a larger signal-to-noise ratio than using the integrated signal and it was used in measurements involving smaller films in this work. One slightly different approach employs a large alternating field applied near the hard direction and provision for physically rotating the film small angles with respect to the applied field. The apparent dispersion is found by assuming that regions where the magnetization has an easy direction which makes less than a 90^o angle with the applied field rotate coherently while regions where the magnetization which has an easy direction at greater than 90^o give no net magnetization in the longitudinal direction.

Note that the data illustrated in Figure 3 shows a definite increase in apparent dispersion as the size of the sample decreases. This phenomenon has been noted, but no reason has been shown for it. It should not be comforting to those who embrace the model of non-interacting regions with

different anisotropy directions to note that where the inhomogeneities should have the greatest effect, the apparent dispersion is actually the least.

Measurements of apparent amplitude dispersions have been made by using a common M-H checker (5) and by using magneto-resistance measurements (8) to determine the transverse characteristics of a film. If the magnetization in a film is in a remanent state, the application of a transverse field rotates the magnetization as a single domain only to a critical angle ϕ_c. A further increase in transverse field eventually demagnetizes the film to a state where half the magnetization has an easy direction antiparallel to the other half. A typical model used to interpret the results of this experiment might assume that different regions in the film have different values of H_k and that increasing the transverse field h_T from h_T to $h_T + \Delta h_T$ causes the magnetization in regions where H_k obeys the relationship $h_T < H_k < h_T + \Delta h_T$ to demagnetize into a state where half the region has an easy direction antiparallel to the other half. More complicated schemes can be used which allow for both angular and magnitude dispersions. The results of two independent experiments are then used to find the apparent distributions of α and H_k. Torok and others (7) use the opening of a small-signal easy-direction hysteresis loop as a transverse bias field is changed and as the film is rotated to determine the distributions.

II. THEORY

A. Demagnetizing Fields

The magnetic flux density $\underline{B}$ may be defined in terms of current density $\underline{j}$ as (4),

$$\underline{B} = \frac{\mu_o}{4\pi} \int_{\text{All Space}} \frac{\underline{j} \times \underline{r}}{r^3} \, dv \quad ,$$

where μ_o is the permeability of free space and $\underline{r}$ is the displacement from the differential volume dv to the point of observation. Difficulty would be encountered in direct calculation of $\underline{B}$ in the vicinity of materials because of atomic current densities. This difficulty is partially overcome by the concept of magnetization $\underline{M}$. The magnetization of a material is the effective flux density which would exist in an infinite sample of the substance because of atomic current densities. The magnitude of $\underline{M}$ is about 1 weber/m^2 for 80-20 Ni-Fe permalloy. Hence, $\underline{M}$ is a function of the current densities at the point of interest. Now another quantity $\underline{H}$ may be defined such that $\underline{B} = \mu_o \underline{H} + \underline{M}$. The nature of $\underline{H}$ may be found by noting that $\nabla \cdot \underline{B} = 0$ and $\nabla \times \underline{B} = \mu_o \underline{j}$. This implies that $\nabla \times \underline{H} = \underline{j}_o$ and $\nabla \cdot \underline{H} = -1/\mu_o \nabla \cdot \underline{M}$, where $\underline{j}_o$ is the current density except atomic current density. The problem of finding $\underline{H}$ if current $\underline{j}_o$ is zero is equivalent to finding $\underline{E}$ in an electrostatic system and $-\nabla \cdot \underline{M}$ would correspond to a magnetic charge density. This $\underline{H}$ is called the demagnetizing field, and its value depends on discontinuity of the magnetization.

Regions in a material in which the magnetization is uniform are

called domains, and boundaries between domains are called domain walls. The magnetization in thin magnetic films is constrained to lie in the plane of the films because of magnetostatic energy, as may be envisioned easily through a parallel-plate-capacitor analogy. A rotation of $\underline{M}$ with an angle ϕ out of the plane of the film causes a surface pole density of $M \sin\phi$ on one surface and $-M \sin\phi$ on the other surface. The demagnetizing field would then be $M \sin\phi/\mu_o$, and a restoring torque per unit volume of $M^2 \sin\phi \cos\phi /\mu_o$ would result. For 80-20 Ni-Fe permalloy an angle of 10^{-2} radian would correspond to a torque per unit volume of roughly 10^4 newton-meters/m^3. In order for an equivalent torque to be produced by an external field applied at 90 degrees to $\underline{M}$, the field would need to be 120oe. Hence, even relatively small angles of rotation out of the plane of the film cannot occur without the application of large fields normal to the plane of the film. The demagnetizing fields in thin magnetic films may be calculated if the domain structure and film geometry are known. However, for even the most simple geometries and domain structures, the calculation is very difficult. It was necessary to find a useful approximation for round films.

The one geometric volume of constant magnetization which has a uniform demagnetizing field is the ellipsoid. This would not be particularly relevant to the calculation of the demagnetizing field inside a flat disc but for the fact that the magnetization need not be uniform in the disc. As a matter of fact, $\underline{M}$ cannot be directed normal to the edge of the film near the edge because the demagnetizing field would be about 5000oe, or several orders of magnitude larger than known coercive fields for 80-20 Ni-Fe

permalloy. Domain patterns invariably show "spike" domains at film edges where $\underline{M}$ is directed along the edges. As an approximation the free pole distribution in a disc is assumed to be the same as the free pole distribution in an equivalent ellipsoid of revolution of constant magnetization having the same diameter as the disc. That is, the magnetic charge in a differential surface area in the disc is assumed to be the same as the magnetic charge projected from $-\nabla \cdot \underline{M}$ on the surface of a flat ellipsoid of revolution. Under this assumption Appendix A derives the relationship between the demagnetizing field H_D and ϵ, the percentage of saturation magnetization in the direction of average magnetization. The result is illustrated in Figure 5. h_{Lc} is the field $0.785tM/2a\mu_o$, where t is the thickness of the disc and a is the radius of the disc.

B. Magnetization Buckling

Perhaps the chief reason the effects of demagnetizing fields have been generally ignored is that demagnetizing fields exert small torques in single-domain films because the magnetization and the demagnetizing field are nearly antiparallel. The net torque on a magnetic sample due to its demagnetizing field must be zero by conservation of energy. If the magnetization were constrained to a single domain, the effect of demagnetizing fields would be small; however, if allowance is made for wall formation, demagnetizing fields become most important.

Consider the measurement of apparent magnitude dispersion. By using a simple model Thomas (6) has shown that magnetization buckling (or demagnetization in the manner illustrated in Figure 6a) will occur in films having no dispersion of physical properties. The same result will be shown

Figure 5. Calculated relationship between e and H_D.

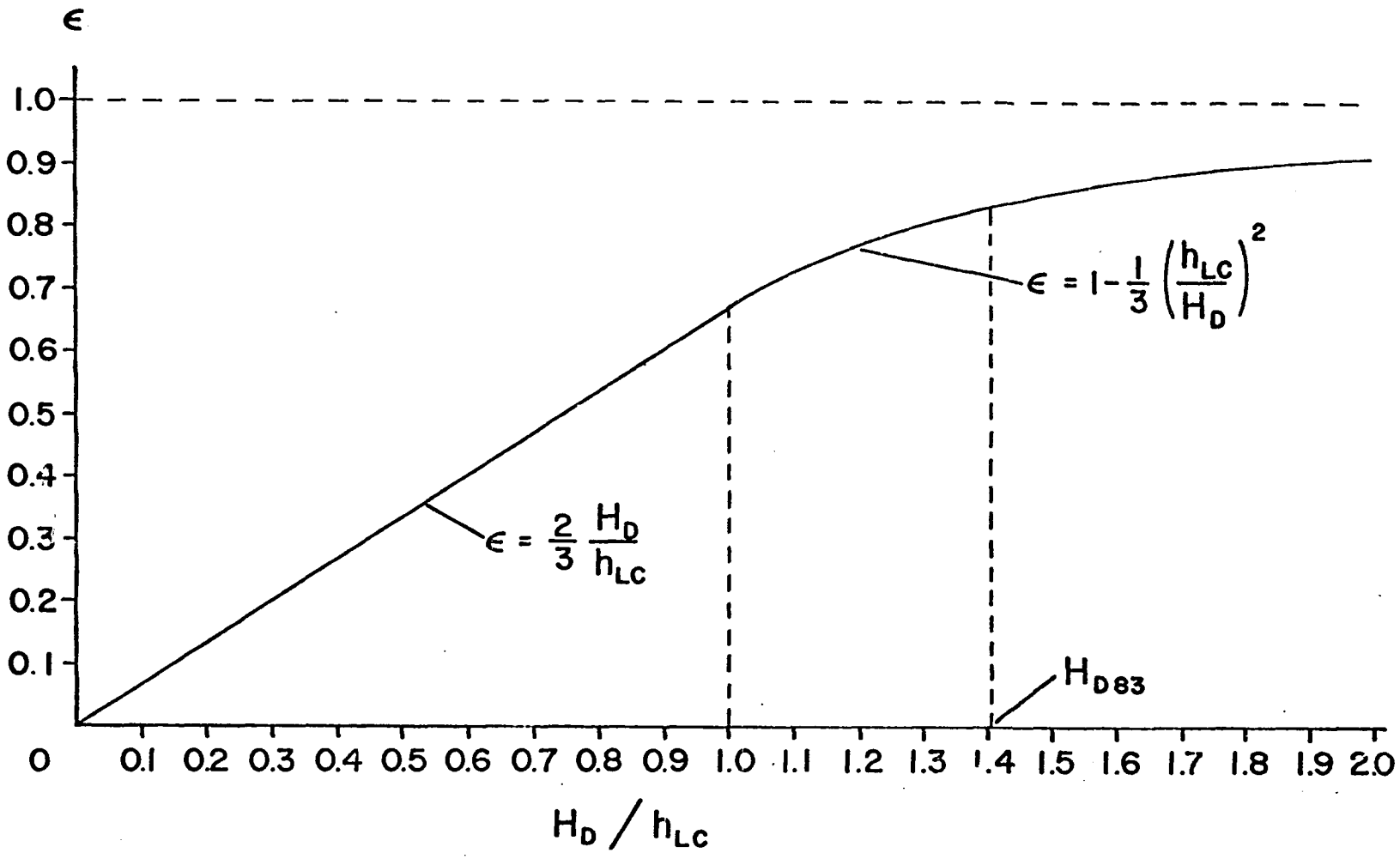
ϵ
1.0
0.9
0.8
0.7
0.6
0.5
0.4
0.3
0.2
0.1
0
0.1 0.2 0.3 0.4 0.5 0.6 0.7 0.8 0.9 1.0 1.1 1.2 1.3 1.4 1.5 1.6 1.7 1.8 1.9 2.0
H_D / h_{LC}
$\epsilon = \frac{2}{3} \frac{H_D}{h_{LC}}$
$\epsilon = 1 - \frac{1}{3} \left(\frac{h_{LC}}{H_D} \right)^2$
H_{D83}

Figure 6. Buckling model and resulting relationship between ϵ and h_T.

a) Buckled film.

b) Relationship between ϵ and h_T.

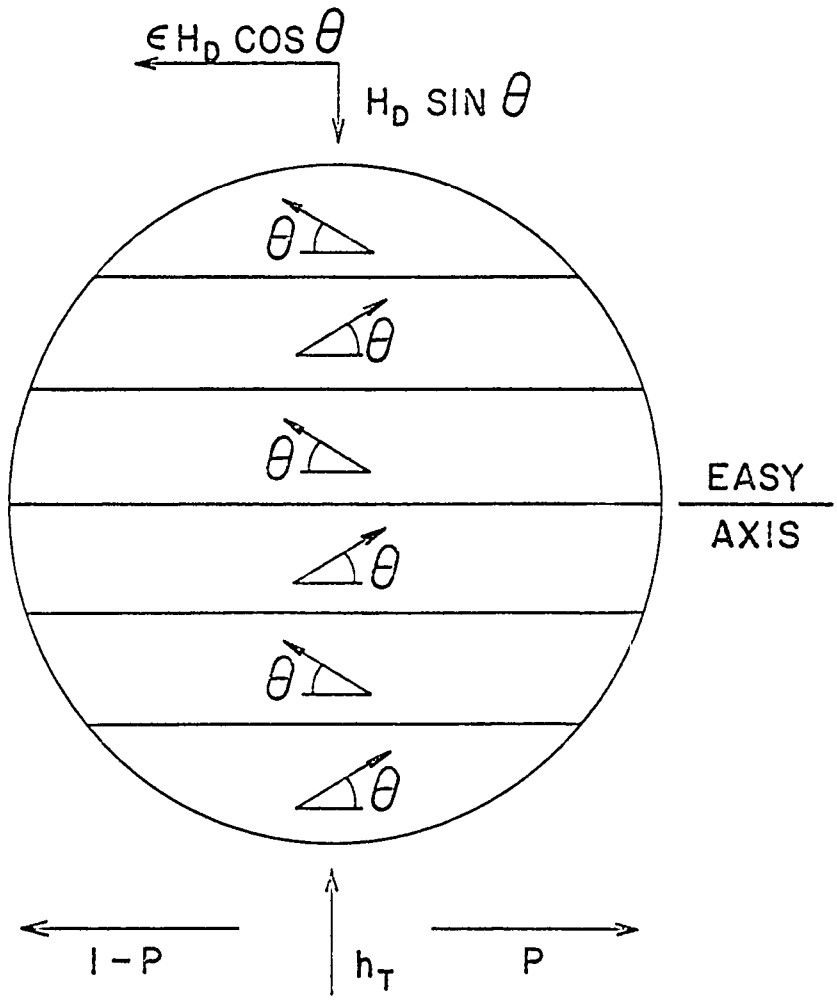
$\epsilon H_D \cos\theta$
$H_D \sin\theta$
θ
EASY
AXIS
1 - P
h_T
P

(a)

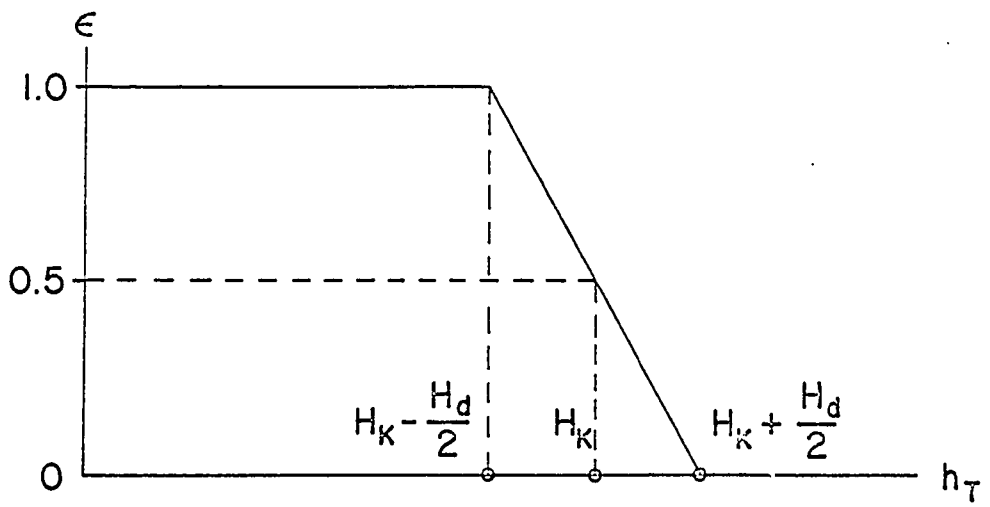
ϵ
1.0
0.5
0
$H_K - \frac{H_d}{2}$
H_{K1}
$H_K + \frac{H_d}{2}$
h_T

(b)

here using a somewhat different model. Let a transverse field h_T be applied to a film as illustrated in Figure 6a. Suppose the demagnetizing field is a constant in the film and let H_D be the magnitude of the demagnetizing field which exists when the film is a single domain. Suppose the film demagnetizes in long strips and let P be the fraction of magnetization which has an easy-direction to the right and 1-P be the fraction of magnetization which has an easy-direction to the left. The hard direction component of demagnetizing field is then $H_D \sin \phi$ and the easy direction component is $(2P-1) H_D \cos \phi = \epsilon H_D \cos \phi$. The torque T per unit volume on the regions where the easy direction is to the right is

$$T = M(h_T \cos \phi - H_k \sin \phi \cos \phi + \epsilon H_D \sin \phi \cos \phi - H_D \sin \phi \cos \phi)$$

$$M[h_T \cos \phi - H_k' \sin \phi \cos \phi], \text{ where } H_k' = H_k - (1-\epsilon) H_D.$$

If the torque is zero, then

$$\sin \phi = \frac{h_T}{H_k}.$$

There is a restoring torque per unit volume T_R tending to return the magnetization to the equilibrium position after a small angular displacement $\Delta\phi$ given by

$$T_R = \frac{\partial T}{\partial \phi} \Delta\phi = M[h_T \sin \phi + H_k' \cos 2\phi].$$

There is also a "buckling torque" T_B due to the demagnetizing field which tends to rotate the magnetization away from equilibrium.

$$T_B = M H_D \sin^2 \phi + \epsilon H_D \cos^2 \phi \Delta\phi .$$

This torque is the important factor. If the magnetization were a single domain ($\epsilon = 1$), then $T_B = MH_D \Delta\phi$. Note that if $T_B > T_R$ the magnetization is in a state of unstable equilibrium, and any slight disturbance would switch part of the magnetization until, because of the reduction of ϵ, the demagnetizing field decreases sufficiently to let $T_R = T_B$. Hence, ϵ will adjust so that

$$h_T \sin \phi + H_k' \cos 2\phi = H_D \sin^2 \phi + \epsilon H_D \cos^2 \phi .$$

Letting $h_T = H_k' \sin \phi$,

$$H_k' \cos^2 \phi = H_D \sin^2 \phi + \epsilon H_D \cos^2 \phi .$$

Dividing by $\cos^2 \phi$ and rearranging gives

$$\tan^2 \phi = \frac{H_k' - \epsilon H_D}{H_D} = \frac{H_k - H_D}{H_D} ,$$

or

$$\sin^2 \phi = 1 - H_D/H_k$$

and

$$\sin \phi = \sqrt{1 - \frac{H_D}{H_k}} .$$

This angle is probably close to the angle of irreversible rotation ϕ_c. If $H_D/H_k \ll 1$, ϵ is found to be unity for $h_T \leq H_k - H_D/2$, and ϵ decreases linearly to zero at $h_T = H_k + H_D/2$. The plot of ϵ as a function of h_T is shown in Figure 6b. As is pointed out in Appendix B, these results may

also be found graphically from a switching asteroid. Because non-uniform demagnetizing fields exist in all but ellipsoidal samples, there are probably different critical angles at which irreversible rotation takes place in different regions of the film.

Although the energy necessary to form domain walls has been neglected, an argument for the occurance of magnetization buckling and apparent magnitude dispersion in films with no dispersions of physical properties has been presented.

C. Angular Dispersion

The previous section presents a mechanism for domain formation which does not rely on physical inhomogeneities in the film. This section presents two simple mechanisms by which the angular dispersion measurement described in the Introduction might be explained without resorting to an actual dispersion of the easy axis. The two models give the fraction of the saturation magnetization in the easy direction ϵ as a function of a small easy-direction field h_L when a large alternating transverse field is applied. The rotational model is similar to the magnetization buckling model in that the demagnetizing field adjusts with h_L to keep that part of the film with an easy direction parallel to h_L barely stable as h_T decreases to zero. The wall motion model assumes that the walls in a "buckled" film are very sensitive to longitudinal fields when the transverse field is small, and that in fact the walls may move to make the net longitudinal field zero, i.e., the applied field h_L is cancelled by a demagnetizing field H_D. For both models the demagnetizing field is assumed to obey the relationship derived in Appendix A for ϵ and H_D.

Analyzing the rotational mechanism requires solving for instability of the magnetization by setting first and second derivatives of the total energy to zero and solving the equations simultaneously. The algebraic solution to these equations is difficult. The graphical approach which uses the switching asteroid as outlined in Appendix B is not too difficult. For a given film h_{LC} may be found. Then corresponding to an ϵ an H_D may be found. Two methods of using H_D were tried. One assumed that the magnetization on the interior of the circle rotates coherently with a demagnetizing field H_D corresponding to the relationship illustrated in Figure 5. The results using this method are similar to the results obtained from using a second method, and details of only the second method are discussed here. The film is considered made up of two parts, one with an easy direction anti-parallel to the other. Each part is considered to furnish its own demagnetizing field. The demagnetizing field is then the difference between these fields as the magnetizations are near the easy axis and the sum of the two when the magnetizations are near the hard axis. The demagnetizing field which exists when the magnetizations are near the easy direction is taken from Figure 5. Hence, if $\epsilon = 0.83$, the demagnetizing field is 1.41 h_{Lc} when the magnetizations are near the easy axis and $1.41\ h_{Lc}/0.83 = 1.7\ h_{Lc}$ when the magnetizations are near the hard direction. H_D is decomposed into two components antiparallel to the two magnetizations. If the two magnetizations make a small angle with each other, the magnitudes of the components are about $\frac{1+\epsilon}{2} H_D$ and $\frac{1-\epsilon}{2} H_D$. The asteroid may then be used to find the smallest value of h_L which does not permit the magnetization to become unstable as it rotates from the hard direction

to the easy direction. Using this procedure leads to an ϵ as a function of h_L which is illustrated in Figure 7. h_L is expressed as multiples of H_K, the anisotropy field, and h_{Lc}/H_K is a parameter. The apparent dispersion angle α_{83} may be found from this relationship as $\alpha \simeq h_{L83}/H_K$ where h_{L83}/H_K is the point which corresponds to $\epsilon = 0.83$. Figure 8 gives h_L/H_K as a function of H_D/H_K with ϵ as a parameter.

The analysis of the wall-motion mechanism is not difficult once the relationship between ϵ and H_D has been determined since this model assumes $h_L = H_D$. Figure 9 shows the relationship between h_L and ϵ, which is actually only a relabeling of the H_D axis of Figure 5.

Figure 7. Relationship between ϵ and h_L/H_K with h_{Lc}/H_K a parameter calculated from the rotational model.

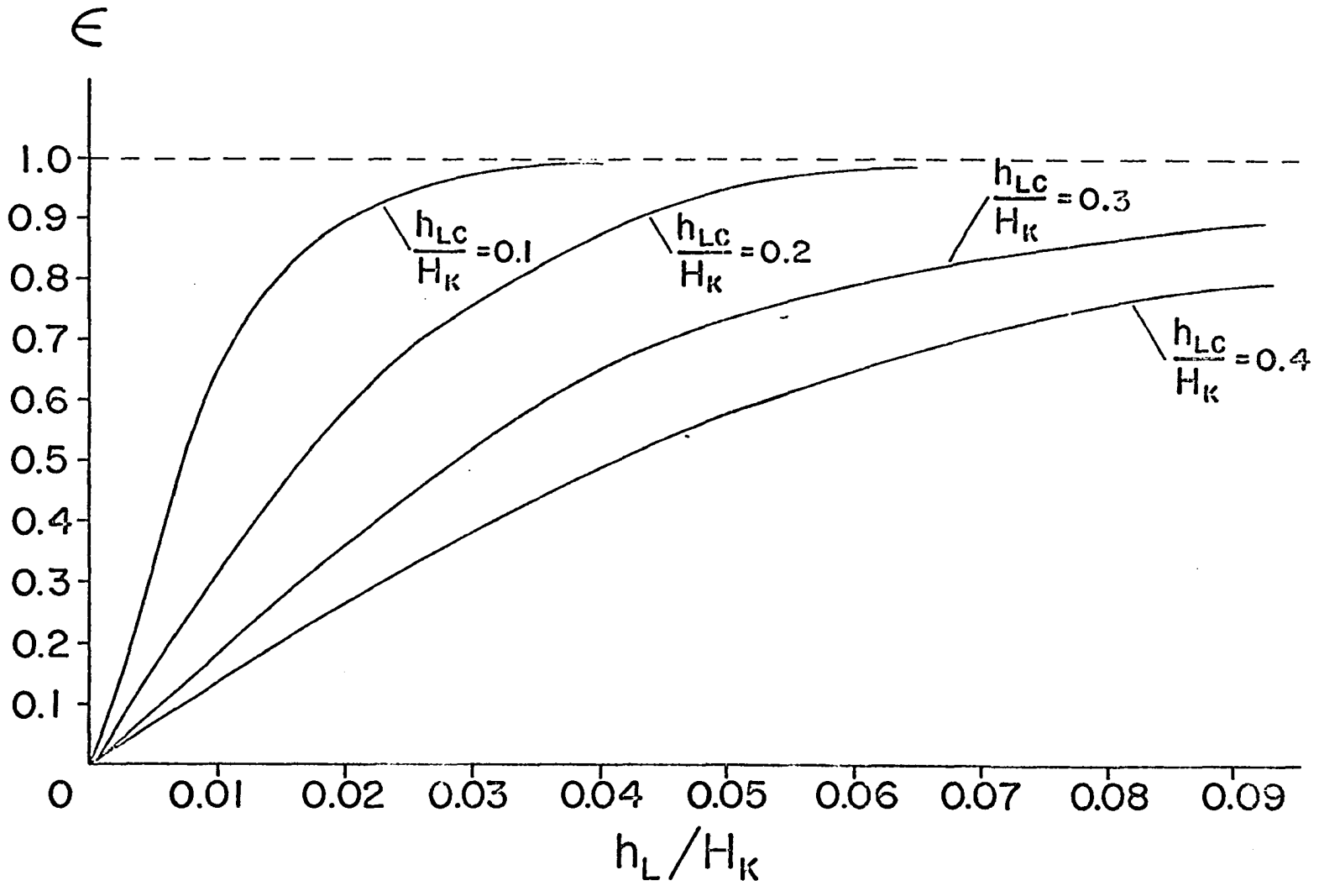
ϵ
1.0
0.9
0.8
0.7
0.6
0.5
0.4
0.3
0.2
0.1
0
0.01
0.02
0.03
0.04
0.05
0.06
0.07
0.08
0.09
h_L/H_K
$\frac{h_{LC}}{H_K}=0.1$
$\frac{h_{LC}}{H_K}=0.2$
$\frac{h_{LC}}{H_K}=0.3$
$\frac{h_{LC}}{H_K}=0.4$

Figure 8. Relationship between h_L/H_K and H_D/H_K with ϵ as a parameter as calculated from the rotational model.

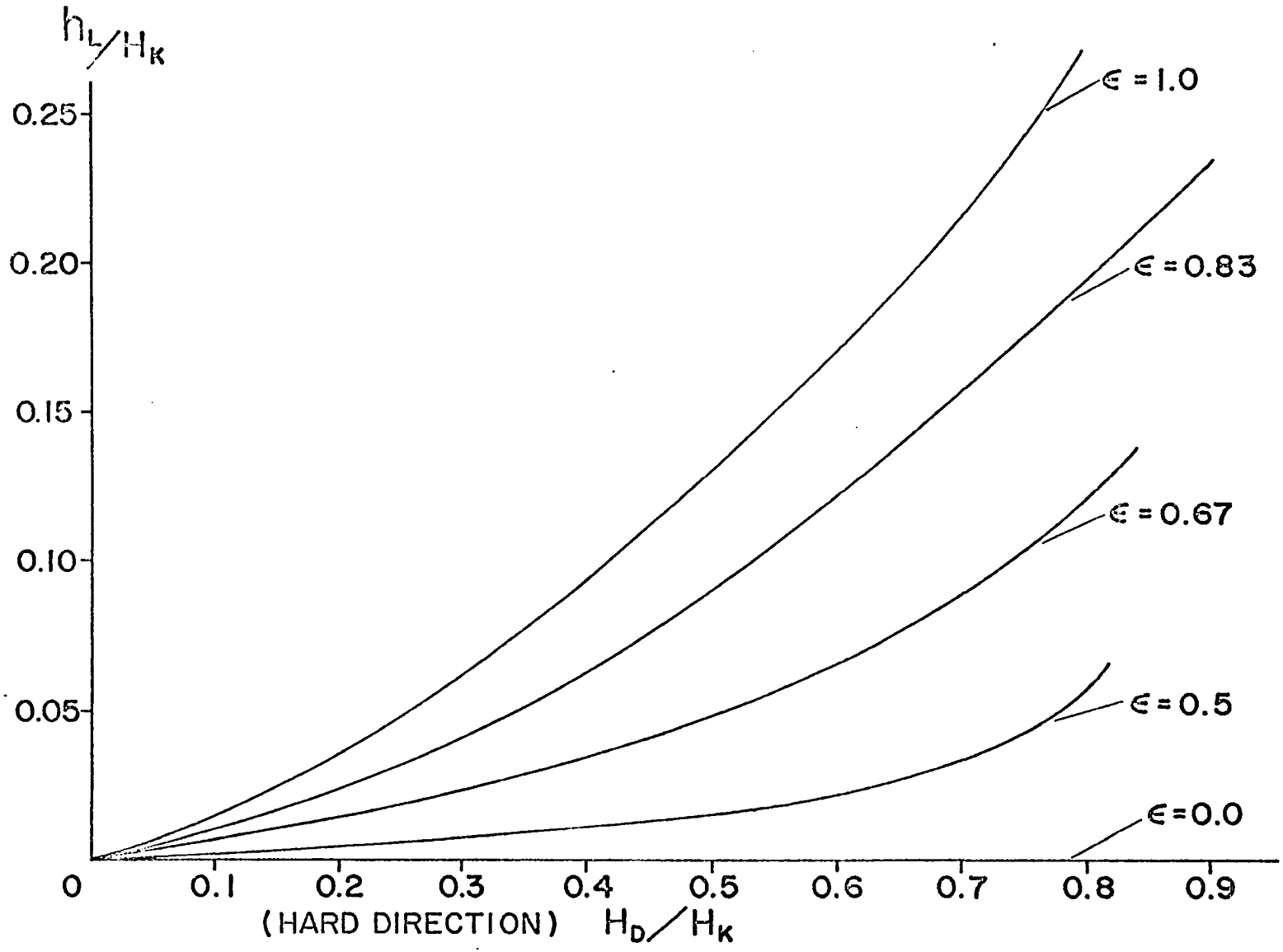
h_L/H_K
0.25
0.20
0.15
0.10
0.05
0
0.1
0.2
0.3
0.4
0.5
0.6
0.7
0.8
0.9
(HARD DIRECTION) H_D/H_K
$\epsilon = 1.0$
$\epsilon = 0.83$
$\epsilon = 0.67$
$\epsilon = 0.5$
$\epsilon = 0.0$

Figure 9. ϵ as a function of h_L calculated from the wall motion model.

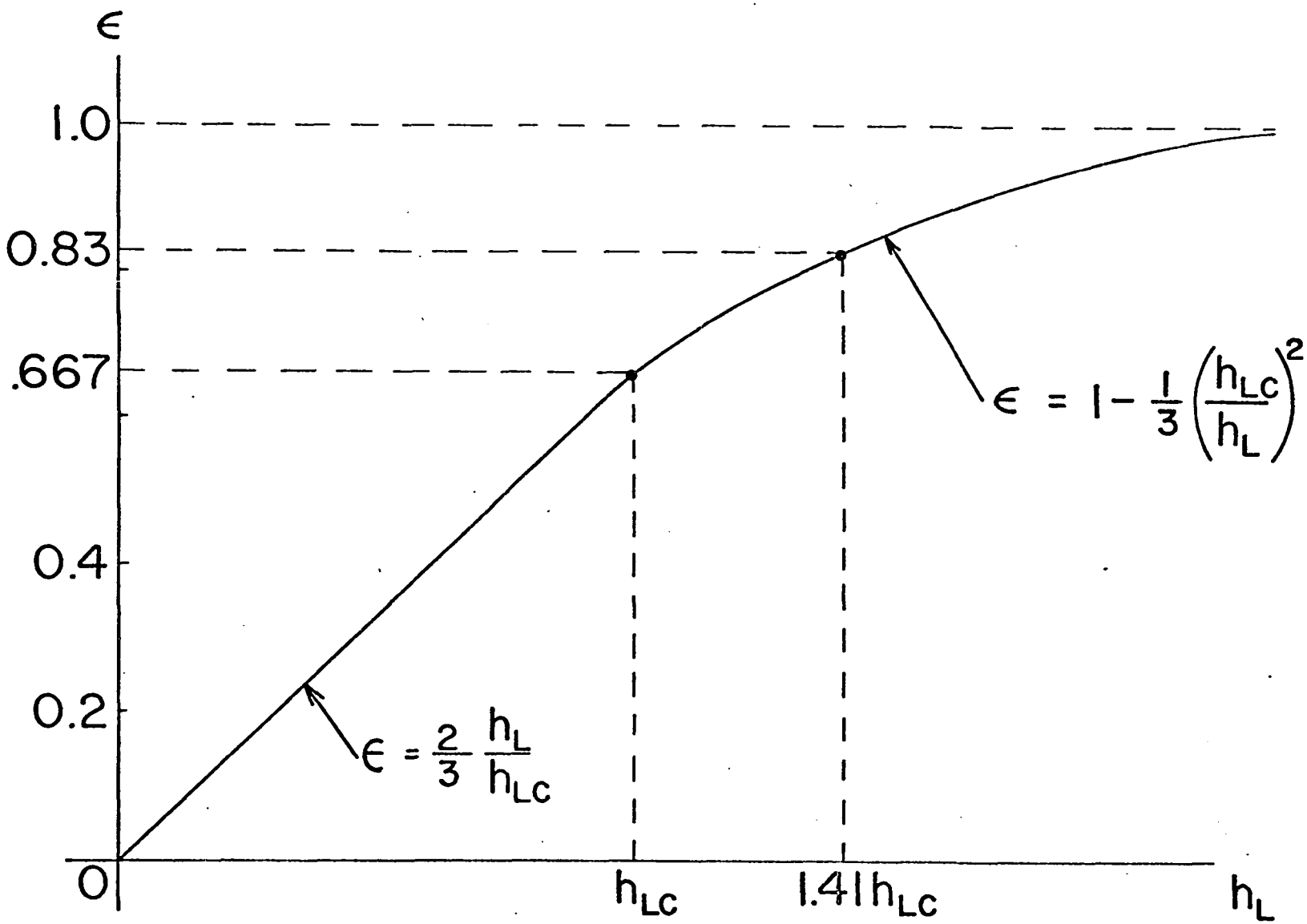
ϵ
1.0
0.83
.667
0.4
0.2
0
h_{LC}
$1.41 h_{LC}$
h_L
$\epsilon = \frac{2}{3} \frac{h_L}{h_{LC}}$
$\epsilon = 1 - \frac{1}{3}\left(\frac{h_{LC}}{h_L}\right)^2$

III. EXPERIMENTAL DATA

The basic method of measuring apparent angular dispersion which was described in the Introduction was used to make measurements on many films. The results illustrated in Figure 3 and Figure 4 are typical.

Data for dispersion as a function of demagnetizing fields was desired to determine the validity of the theoretical models. In trying to measure apparent dispersions for a wide range of demagnetizing fields, noise difficulty was encountered for large demagnetizing fields (which correspond to small films). This difficulty was overcome by filtering the second harmonic of the derivative of the longitudinal flux and by taking ϵ as the ratio of signal output to maximum signal output. This scheme gave the same values for dispersion as the method using the integrated signal for a number of larger films. Data for ϵ as a function of h_L are shown in Figure 10. This method of presenting data on an oscilloscope was suggested by Dr. Thomas Long of the Bell Telephone Laboratories. The large transverse field was about 500 cps while h_L varied at about 3 cps.

All thickness measurements were made by comparing the saturation flux to the saturation flux of a standard film. It was noted experimentally that the "shear" on the easy-direction hysteresis loop was not a reliable measure of the demagnetizing field.

Data on a number of films are illustrated in Figure 11. The two film series were cut from two larger films; therefore the physical properties of the films in the series should have been reasonably uniform.

These results seemed favorable, but they dealt with films of only one

Figure 10. Oscilloscope presentation of apparent dispersion data for three rectangular films.

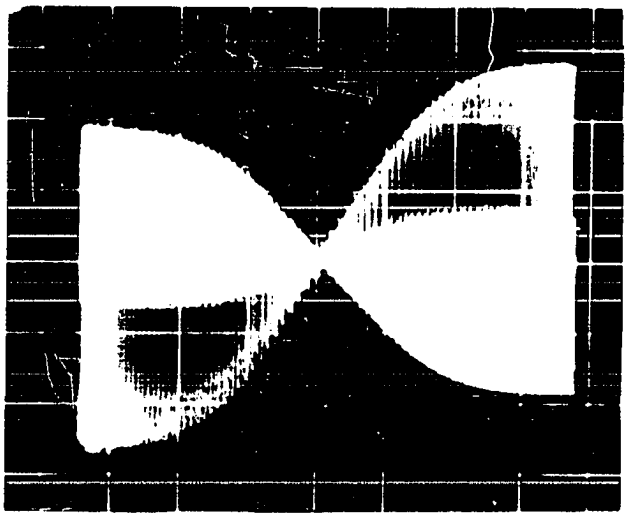

Thickness ~ 2000 A°
10mm x 11mm
H_K ~ 3.3 oe
0.153 oe/div
α_{83} ~ 5°

Thickness ~ 2000 A°
5.1mm x 5.1mm
H_K ~ 3.3 oe
0.153 oe/div
α_{83} ~ 7.5°

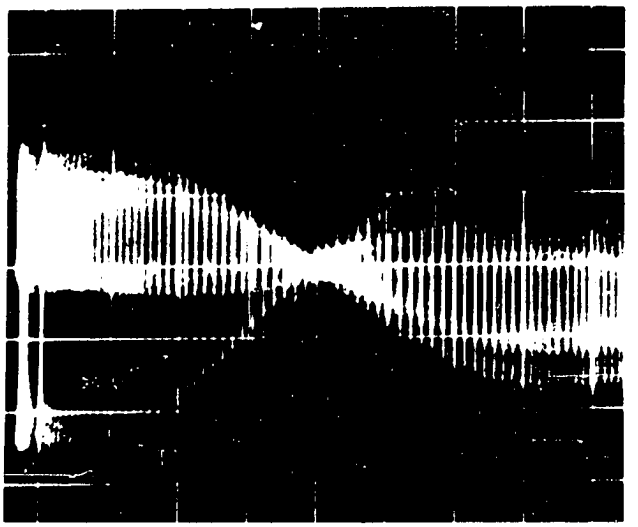

Thickness ~ 2000 A°
1.5mm x 2.1mm
H_K ~ 3.3 oe
0.382 oe/div
α_{83} ~ 17.5°

Figure 11. Data on apparent angular dispersion as a function of demagnetizing field.

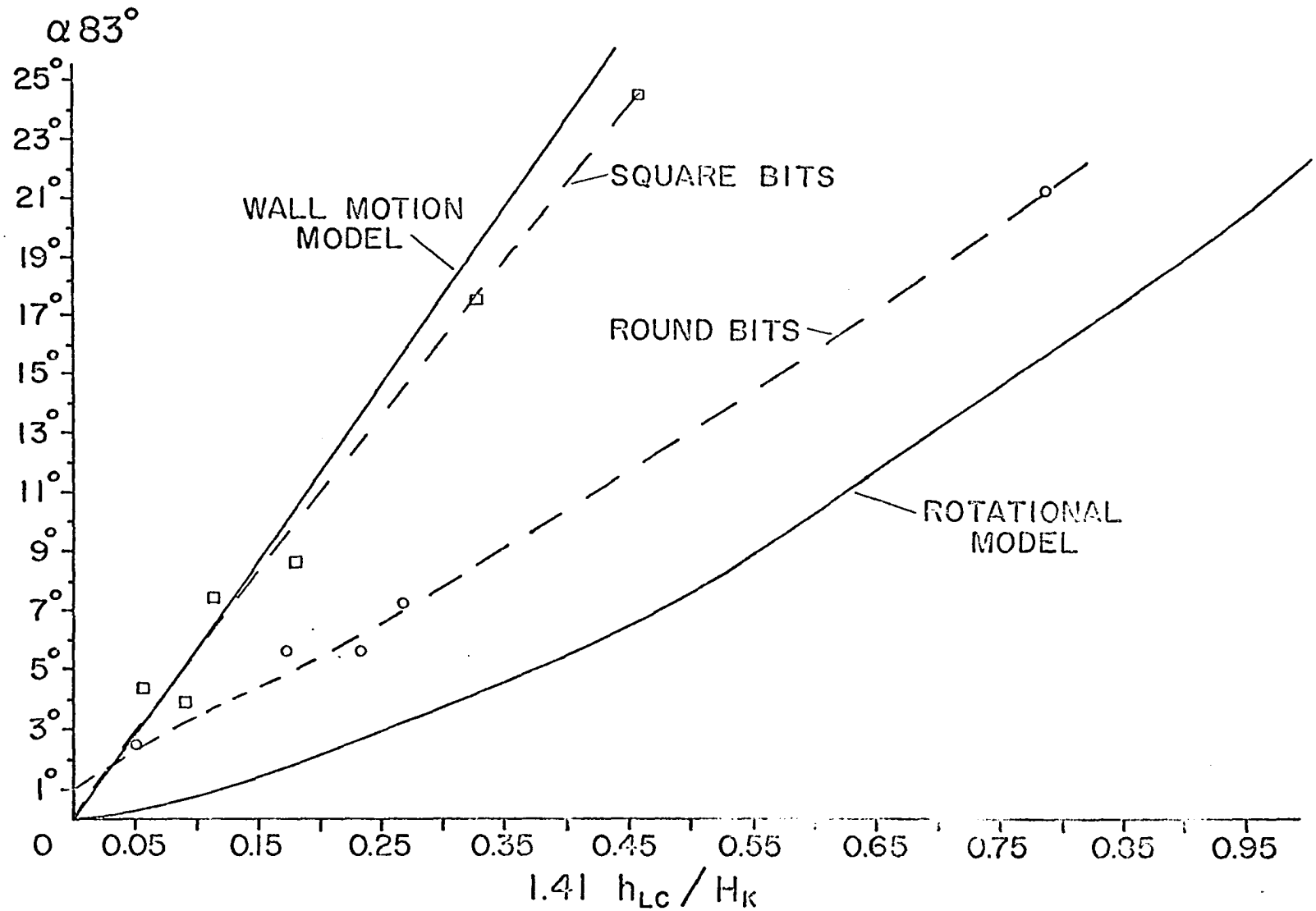
α 83°
25°
23°
21°
19°
17°
15°
13°
11°
9°
7°
5°
3°
1°
0
0.05
0.15
0.25
0.35
0.45
0.55
0.65
0.75
0.85
0.95
1.41 h_{LC} / H_K
WALL MOTION MODEL
SQUARE BITS
ROUND BITS
ROTATIONAL MODEL

thickness and were formed only by cutting with a scribe. To check for possible effects of thickness three evaporations were made under as nearly identical conditions as possible. The resulting evaporations gave films of 1100 A^{o}, 2100 A^{o}, and 4000 A^{o}. To test the effects of different edges, three methods were used to form the circles. Circles were masked, cut with a scribe and etched with nitric acid. Bee's wax was used to protect the etched films. The values of h_{L83} are plotted as functions of assumed demagnetizing fields in Figures 11, 12, and 13. The films of Figure 11 were cut with a scribe, the films of Figure 12 were masked, and the films of Figure 13 were etched. The smaller masked films were noted to have larger values of H_K.

Table 1. Comparison of experimental and theoretical results of Figure 11.

Film Description			α_{83} Apparent Dispersion		
(oersteds)	Thickness A	Size	α_{83} Rotation	α_{83} Wall Motion	α_{83} Experiment
2.5	1800	16mm Diam	0.3^{o}	2.8^{o}	2.6^{o}
2.5	1800	4.5mm Diam	1.8^{o}	10.2^{o}	5.6^{o}
2.5	1800	4.0mm Diam	2.6^{o}	13.8^{o}	5.6^{o}
2.5	1800	2.9mm Diam	3.2^{o}	15.9^{o}	7.2^{o}
2.5	1800	1.0mm Diam	16.0^{o}	53.4^{o}	21.4^{o}
3.3	2000	10mm x 11 mm	0.4^{o}	3.2^{o}	4.5^{o}
3.3	2000	7mm x 6mm	0.8^{o}	5.2^{o}	4.0^{o}
3.3	2000	5.1mm x 5.1mm	1.0^{o}	6.6^{o}	7.5^{o}
3.3	2000	2.9mm x 3.5mm	2.0^{o}	10.5^{o}	8.6^{o}
3.3	2000	1.5mm x 2.1mm	4.3^{o}	19.3^{o}	17.5^{o}
3.3	2000	1.5mm x 1.1mm	7.0^{o}	27.2^{o}	24.6^{o}

Figure 12. Dispersion data for round films cut with a scribe.

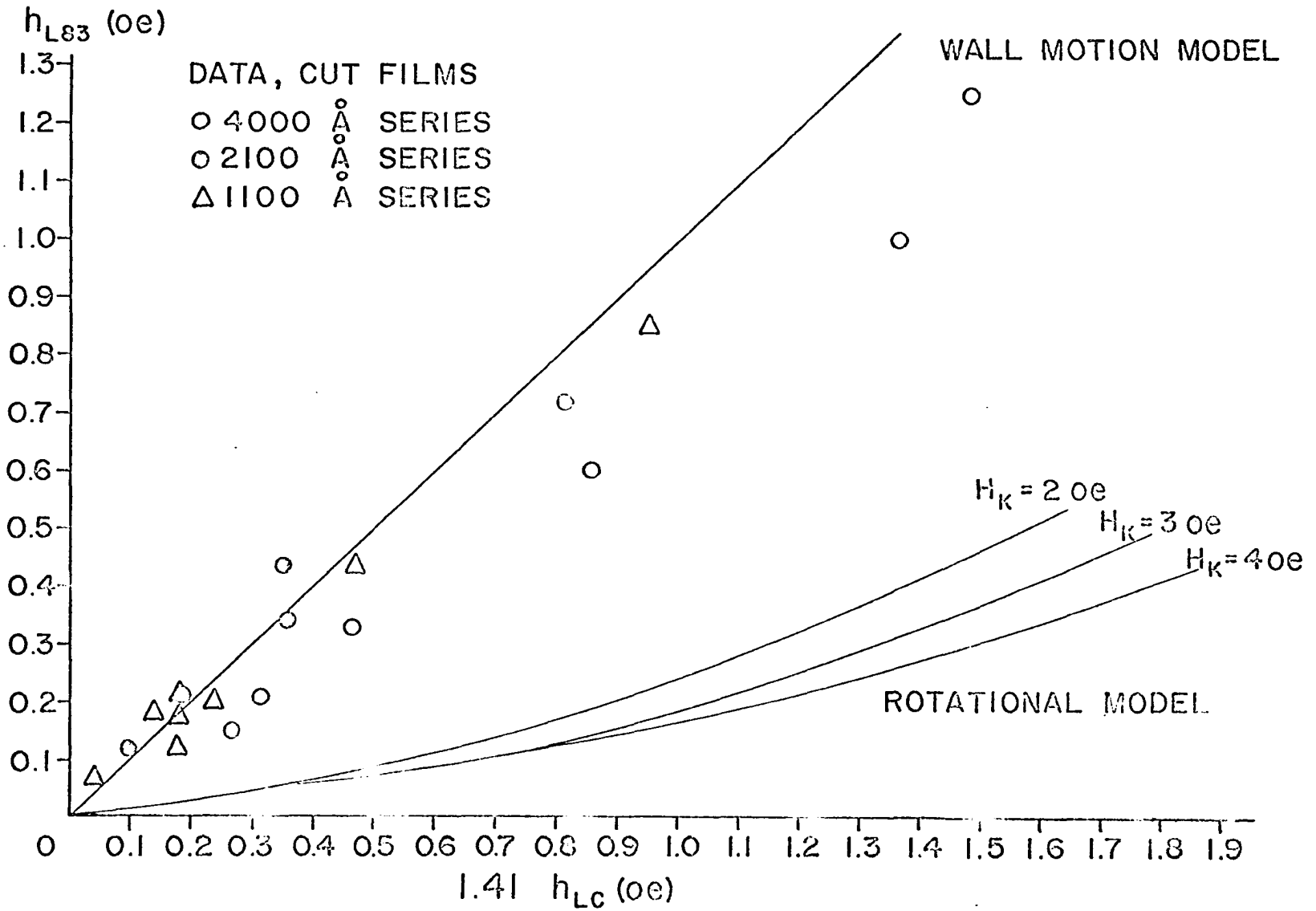
h_{LS3} (oe)
DATA, CUT FILMS
o 4000 Å SERIES
o 2100 Å SERIES
Δ 1100 Å SERIES
WALL MOTION MODEL
H_K = 2 oe
H_K = 3 oe
H_K = 4 oe
ROTATIONAL MODEL
1.3
1.2
1.1
1.0
0.9
0.8
0.7
0.6
0.5
0.4
0.3
0.2
0.1
0 0.1 0.2 0.3 0.4 0.5 0.6 0.7 0.8 0.9 1.0 1.1 1.2 1.3 1.4 1.5 1.6 1.7 1.8 1.9
1.41 h_{LC} (oe)

Figure 13. Dispersion data for round films formed by masking.

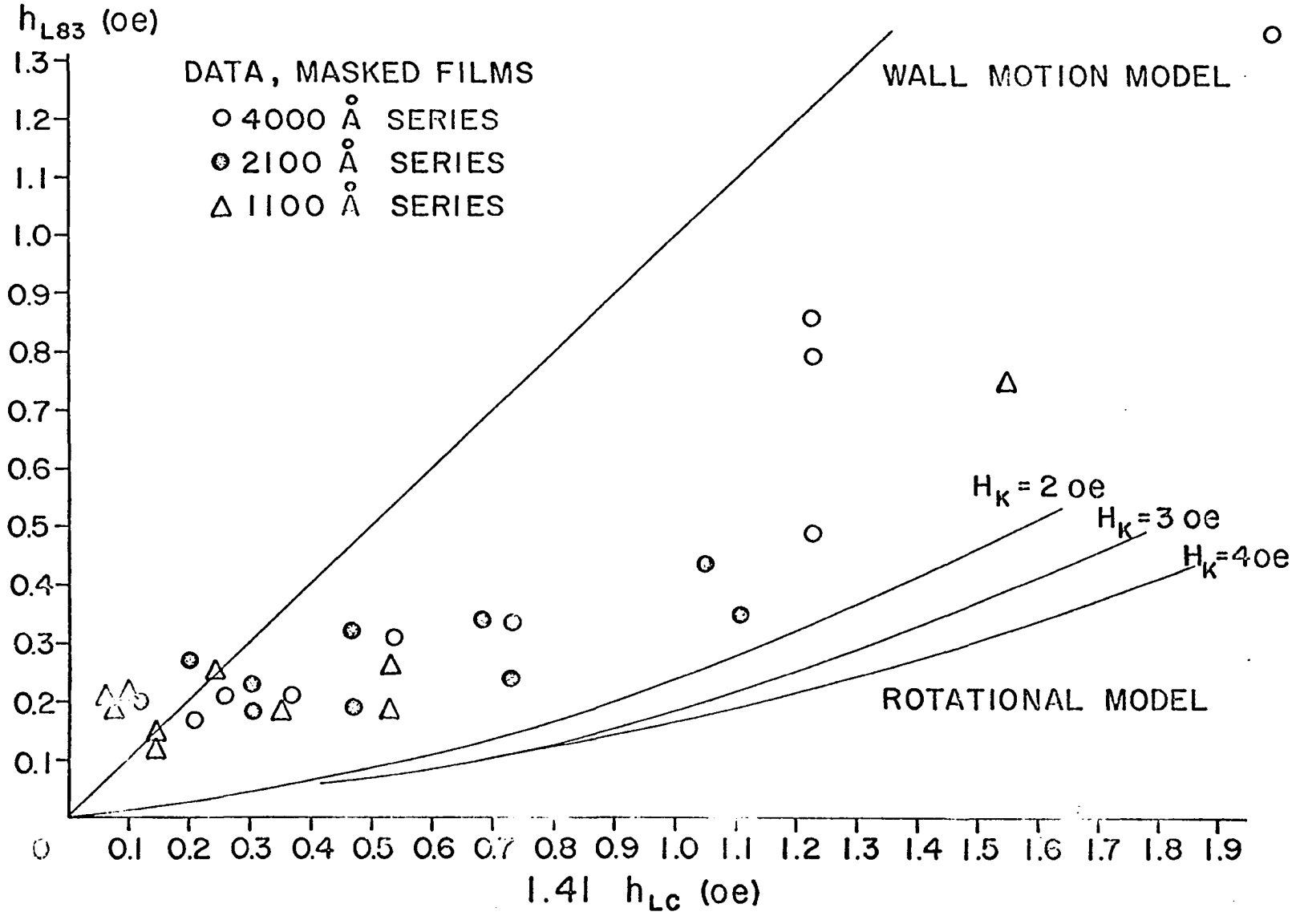
h_{L83} (oe)
DATA, MASKED FILMS
4000 Å SERIES
2100 Å SERIES
1100 Å SERIES
WALL MOTION MODEL
H_K = 2 oe
H_K = 3 oe
H_K = 4 oe
ROTATIONAL MODEL
1.3
1.2
1.1
1.0
0.9
0.8
0.7
0.6
0.5
0.4
0.3
0.2
0.1
0
0.1 0.2 0.3 0.4 0.5 0.6 0.7 0.8 0.9 1.0 1.1 1.2 1.3 1.4 1.5 1.6 1.7 1.8 1.9
1.41 h_{LC} (oe)

Figure 14. Dispersion data for round films formed by etching.

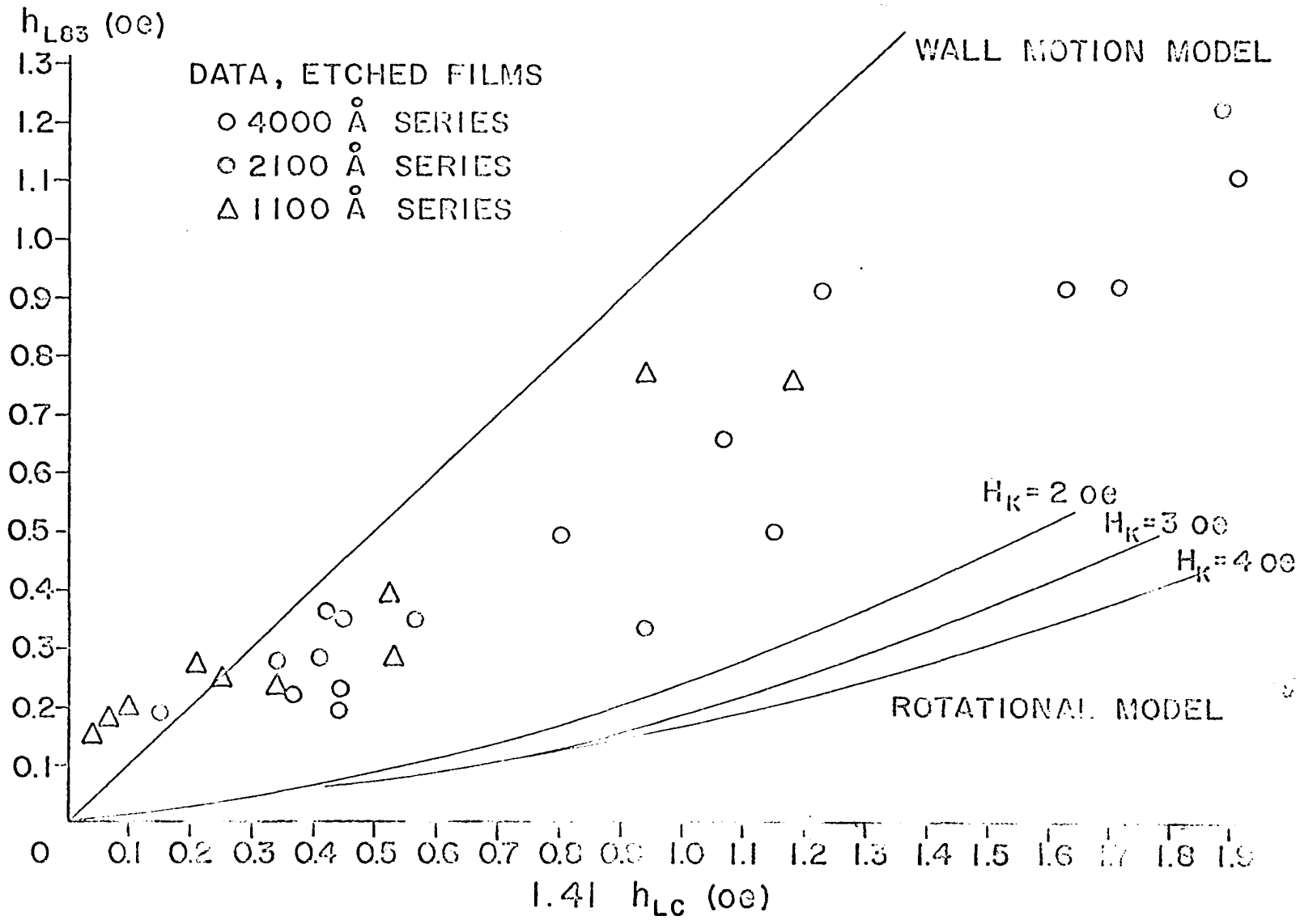
h_{L83} (oe)
DATA, ETCHED FILMS
o 4000 Å SERIES
o 2100 Å SERIES
Δ 1100 Å SERIES
WALL MOTION MODEL
H_K = 2 oe
H_K = 3 oe
H_K = 4 oe
ROTATIONAL MODEL
1.3
1.2
1.1
1.0
0.9
0.8
0.7
0.6
0.5
0.4
0.3
0.2
0.1
0
0.1 0.2 0.3 0.4 0.5 0.6 0.7 0.8 0.9 1.0 1.1 1.2 1.3 1.4 1.5 1.6 1.7 1.8 1.9
1.41 h_{Lc} (oe)

IV. DISCUSSION

The shapes of the ϵ vs. h_L curves which were found experimentally agreed well with the shapes found by the theoretical models.

Probably the most obvious and significant experimental result found in this work is that the apparent angular dispersion does in fact increase with increasing demagnetizing fields. The theoretical curves are plotted as heavy lines along with the data in the previous section. The experimental values of h_{L83} fell nearly without exception between the two curves for a wide variety of films. For very small demagnetizing fields, i.e., for a film radius of about 0.5 cm, the measured "dispersion" was higher than predicted. This is probably due to a real dispersion which could be made less than 1^o with careful film preparation. Excellent results were found for smaller films. There seemed to be a tendancy for the experimental values to approach the rotational model for smaller films. It is possible that this effect was due to the increase in H_K for smaller films. It is more probable that it was due to the increasing difficulty of forming walls as film size decreases, as the work in Appendix C suggests. No clear effects were observed in h_{L83} because of thickness or method of preparing the sample, although the masked samples may have given slightly lower values. In a last-minute private communication with C. H. Tolman and P. E. Oberg of Remington Rand Univac, St. Paul, Minnesota, it was found that they had also come to the conclusion that demagnetizing effects were the most important single factor in determining apparent angular dispersion after they performed a number of carefully-conducted experiments.

One practical application of this work would be in thin film memory

design. The easy-direction field necessary to restore information after a destructive read-out may be estimated, as the wall-motion model places an upper bound and the rotational model a lower bound on the restoring field. Because of the small size of the values of h_L necessary to control a relatively large magnetization, a field sensor has been suggested by Dr. A. A. Read, Iowa State University, which should detect fields of less than 10^{-3} oe.

Further work is suggested in this area. The angle of irreversible rotation θ_c which was found from the buckling model agrees fairly well with published data (2), but the effects of demagnetizing fields on magnitude dispersion measurements should be investigated experimentally. The domain structure in the film during dispersion measurements would be valuable in refining the simple theories presented here.

V. BIBLIOGRAPHY

1. Middelhoek, S. Ferromagnetic domains in thin Fe-Ni films. Amsterdam, Netherlands. Drukkerij Wed. G. Van Soest N.V. 1961.

2. Olmen, R. W. and Rubens, S. M. Angular dispersion and its relationship with other magnetic parameters. Journal of Applied Physics 33: 1107-1109. 1962.

3. Osborn, J. A. Demagnetizing factors for the general ellipsoid. Physical Review 67: 351-357. 1945.

4. Panofsky, Wolfgang K. A. and Phillips, Melba. Classical electricity and magnetism. 2nd ed. Reading, Mass. Addison-Wesley Publishing Company, Inc. 1962.

5. Smith, D. O. and Harte, K. J. Noncoherent switching in permalloy films. Massachusetts Institute of Technology. Lincoln Laboratory. Group Report 53. 1961.

6. Thomas, H. A theoretical model for partial rotation. Journal of Applied Physics 33: 1117-1118. 1962.

7. Torok, E. J., White, A. A., Hunt, A. J., and Oredson, H. N. Measurement of the easy-axis and H_K probability density functions for thin ferromagnetic films using the longitudinal permeability hysteresis loop. Journal of Applied Physics 33: 3037-3041. 1962.

8. West, Forrest G. Magnetoresistance measurements on domain rotation and wall development in Ni-Fe alloy films. Journal of Applied Physics 32: 290S-292S. 1961.

VI. ACKNOWLEDGEMENTS

The author wishes to express his thanks to Dr. A. V. Pohm for his invaluable guidance, to Dr. A. A. Read for his interest and encouragement, to Mr. Chester Comstock for furnishing the switching asteroids, to Mr. William Thomas for doing the drafting, and to Mrs. Sally Zembsch for her help in the final preparation of this thesis.

VII. APPENDIX

A. Calculation of the Demagnetizing Field for Circular Films

Figure 14 shows an ellipsoid of constant magnetization M_o. The surface of the ellipsoid is given by $\frac{x^2 + y^2}{a^2} + \frac{z^2}{c^2} = 1$. The unit normal to the surface $\underline{n}$ is

$$\underline{n} = n_x \underline{a}_x + n_y \underline{a}_y + n_z \underline{a}_z = \frac{\nabla\left(\frac{x^2 + y^2}{a^2} + \frac{z^2}{c^2}\right)}{\left|\nabla\left(\frac{x^2 + y^2}{a^2} + \frac{z^2}{c^2}\right)\right|} = \frac{\frac{x}{a^2}\underline{a}_x + \frac{y}{a^2}\underline{a}_y + \frac{z}{c^2}\underline{a}_z}{\sqrt{\frac{x^2}{a^4} + \frac{y^2}{a^4} + \frac{z^2}{c^4}}}$$

The constant demagnetizing field H_D inside the ellipsoid may be considered due to a surface pole density $M\, n_x$. Imagine distributing the free poles on the surface of the ellipsoid as volumetric pole density ρ in the disc.

$$\rho = \frac{2 M_o n_x}{n_z} = \frac{2M}{t}\frac{c}{a} \quad \frac{x}{\sqrt{a^2 - (x^2 + y^2)}} \; .$$

The relationship which gives the demagnetizing field for extremely flat ellipsoids is found from the work of Osborn (3) as

$$H_D \simeq \frac{0.785}{\mu_o} \frac{c}{a} M_o \; .$$

Hence,

$$\frac{c}{a} = \frac{\mu_o H_D}{0.785 M_o} \; ,$$

and

Figure 15. Ellipsoid of revolution used for calculation of demagnetizing field.

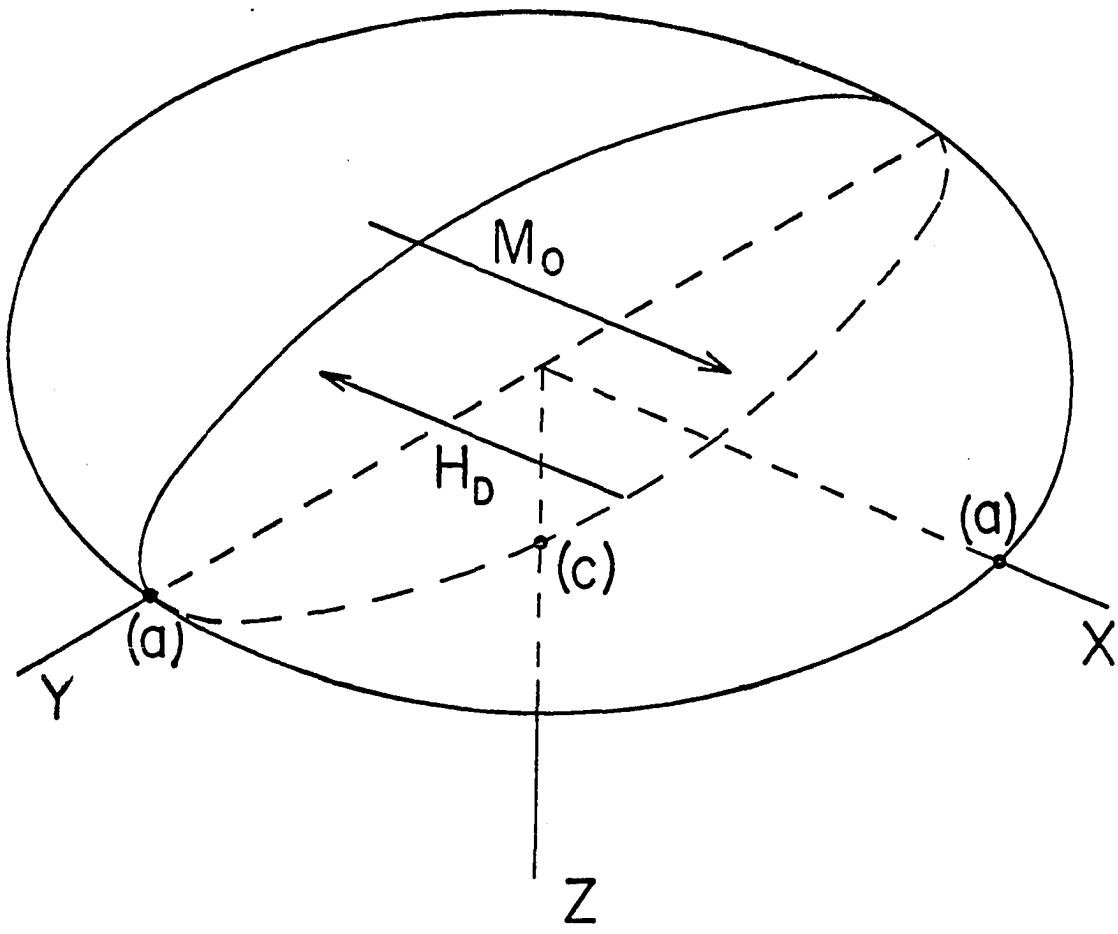

$$\frac{X^2}{a^2} + \frac{Y^2}{a^2} + \frac{Z^2}{c^2} = 1$$

$$\rho = \frac{2\mu_o H_D x}{0.785\ t\sqrt{a^2 - (x^2 + y^2)}}$$

Let the ρ be due to the divergence of M. Assume the net magnetization is in the x-direction only, although it may vary in amplitude.

$$\nabla \cdot \underline{M} = \frac{\partial M}{\partial X} = -\rho$$

$$M = \frac{2\ \mu_o\ H_D}{0.785t}\ \sqrt{a^2 - (x^2 + y^2)}\ .$$

The average magnetization wave may be found by averaging over the sample.

$$M_{ave} = A\frac{\int M dA}{\pi a^2} = \frac{2\ \mu_o\ H_D a}{0.785\ t}\ (\tfrac{2}{3})$$

Note that this relationship cannot hold for sufficiently large h_L because saturation will occur in the center of the film. The critical field h_{Lc} at which the center saturates is found from

$$M_s = \frac{2\ \mu_o\ h_{Lc} a}{0.785\ t}$$

or

$$h_{L_c} = \frac{0.785\ t\ M_s}{2\ \mu_o\ a}\ .$$

Note that at $H_D = h_{Lc}$, $M_{ave} = 2/3\ M_s$. Hence, $\epsilon = 2/3$ at the critical field. Even after the center saturates, not much error should be introduced to M_{ave} by assuming that the demagnetizing field outside the saturated area obeys the same relationships as before saturation. Most of the free pole

concentration is near the perimeter of the circle. Let r_c be the radius of saturation.

$$M_s = \frac{2\mu_o H_D}{0.785t}\sqrt{a^2 - r_c^2}, \text{ and } r_c^2 = a^2\left[1 - \left(\frac{h_{Lc}}{H_D}\right)^2\right].$$

Now suppose that for $H_D > h_{Lc}$, M_{ave} may be calculated from

$$M_{ave} = \frac{\pi r_c^2 M_s + \int_{r_c}^{a} \frac{H_D}{h_{Lc}} a \, M_s \, 2\pi r\sqrt{a^2 - r^2}\, dr}{\pi a^2}$$

$$= M_s\left[1 - \frac{1}{3}\left(\frac{h_{Lc}}{H_D}\right)^2\right]$$

Figure 7 shows a plot of $M_{ave}/M_s = \epsilon$ as a function of H_D. Note that $\epsilon = 0.83$ corresponds to $H_D = 1.41\, h_{Lc}$.

Square films present a more difficult problem. One possible method of modifying the theory presented for round films is to assume a square about $\sqrt{\pi}\, a$ on a side obeys the same relationship for ϵ as a function of H_D as does a round film of radius a. This assumption makes the areas of the square film and the equivalent round film equal.

B. Graphical Solutions Using the Switching Asteroid

Figures 16 and 17 show the switching asteroid and illustrate the manner in which the asteroid may be used to find graphical solutions to problems involving instability of the magnetization. Figure 16 shows, for example, that a ratio $h_L/H_K = 0.14$ allows the magnetization to rotate

Figure 16. Examples of how the switching asteroid may be used to solve graphical problems.

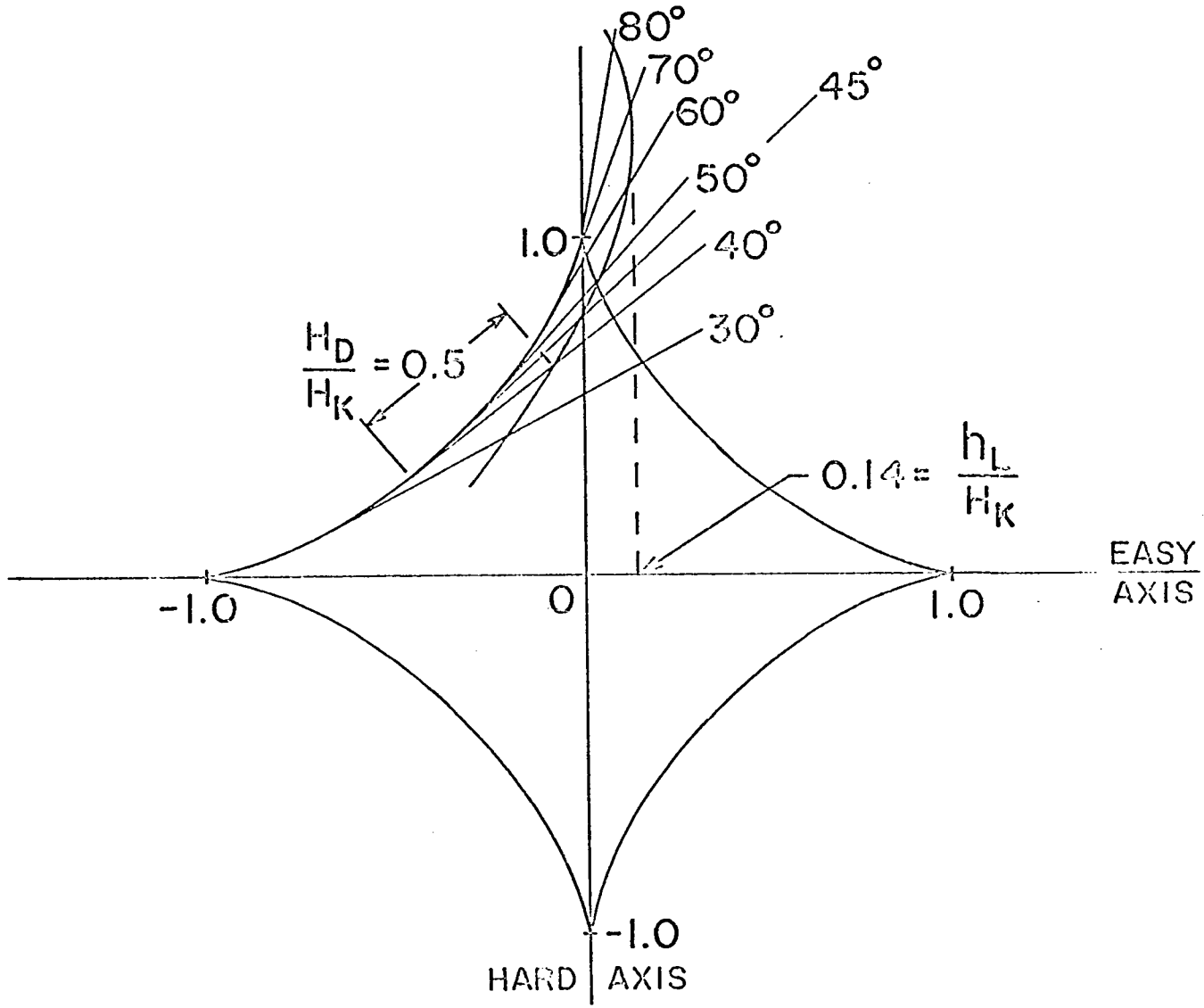
80°
70°
60°
45°
50°
40°
30°
1.0
$\frac{H_D}{H_K} = 0.5$
$0.14 = \frac{h_L}{H_K}$
-1.0
0
1.0
EASY AXIS
-1.0
HARD AXIS

Figure 17. Example of graphical solution to angular dispersion rotational problem using the switching asteroid.

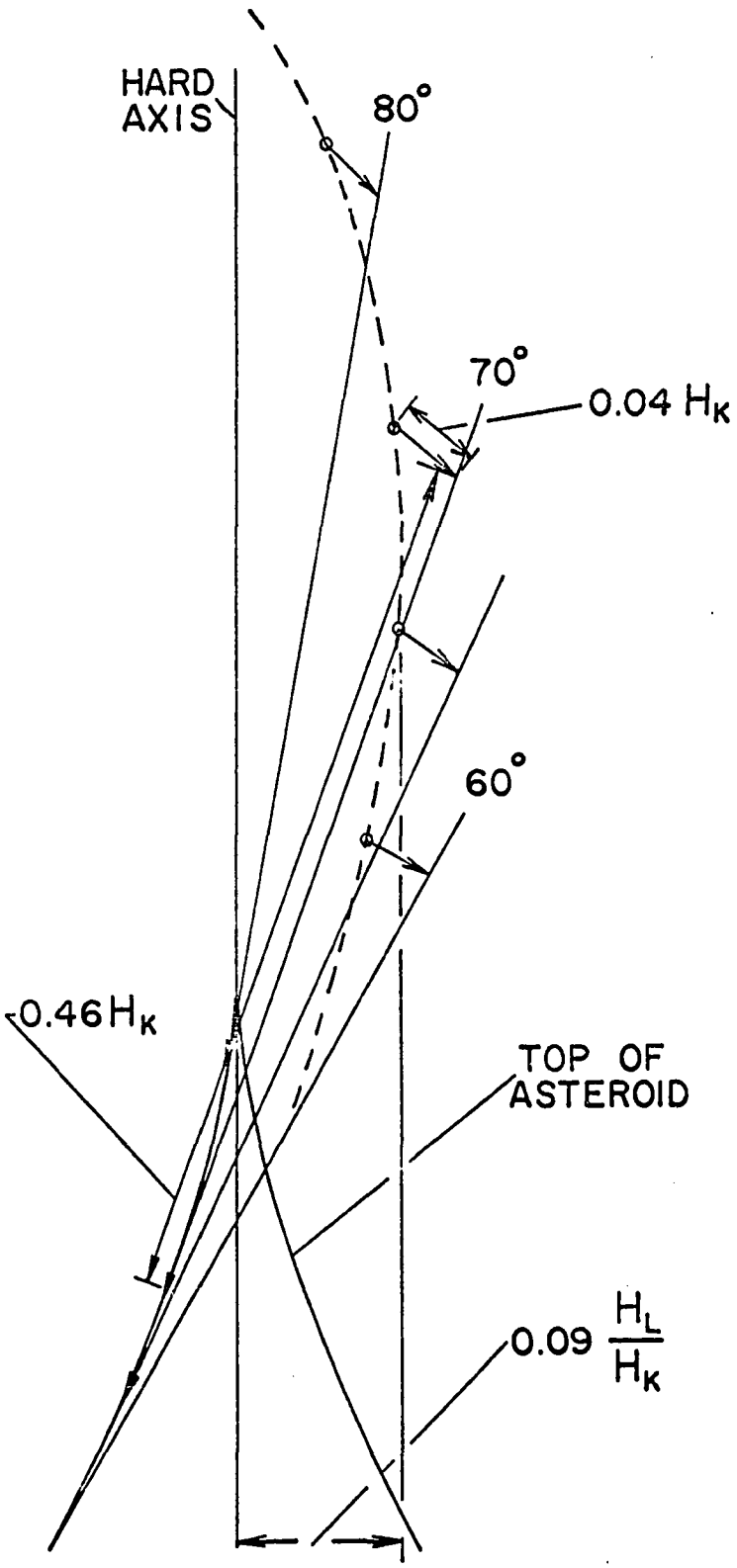
HARD
AXIS
80°
70°
0.04 H_K
60°
0.46 H_K
TOP OF
ASTEROID
0.09 $\frac{H_L}{H_K}$

coherently no matter how large h_T becomes if a demagnetizing field of 0.5 H_K exists. This illustration also shows that $h_L = 0$, a single domain film can rotate coherently to only 45^o. This agrees with the buckling calculation since $\theta_c = \sin^{-1}\sqrt{1 - H_D/H_K} = \sin^{-1}\sqrt{1/2} = 45^o$. Figure 17 does not assume a single domain, but rather $\epsilon = 0.83$. For small angles between the two magnetizations, the demagnetization field H_D may be formed by two components as shown. The magnitude of one component is 0.46 H_K and the other 0.04 H_K to give a net value of about 0.5 H_K. h_{L83} must then be about 0.09 H_K in this case. One of the disadvantages to this type of calculation is that an accuracy better than roughly 10 percent is difficult to obtain.

C. Effect of Size on the Number of Domains in a Film

Because of the wall energy, there is a tendancy for the film to form fewer domains, and hence for ϵ to approach unity for a smaller h_L. Furthermore that this tendancy is probably size sensitive is suggested by the simple model illustrated in Figure 18. The total energy E of this pattern is given by

$$E = LNt\,\sigma_{wall} + \sqrt{2}\,\sigma_{wall}\,Lt + Kt\,\frac{L^2}{2N}$$

where L is the side length, N is the number of parallel strips, t is the thickness of the film, σ_{wall} is the energy per unit cross-section area of the wall, and K is the anisotropy constant. Minimizing E with N,

$$\frac{\partial E}{\partial N} = Lt\,\sigma_{wall} - Kt\,\frac{L^2}{2N^2} = 0\ ,$$

Figure 18. Domain configuration with zero magneto-static energy.

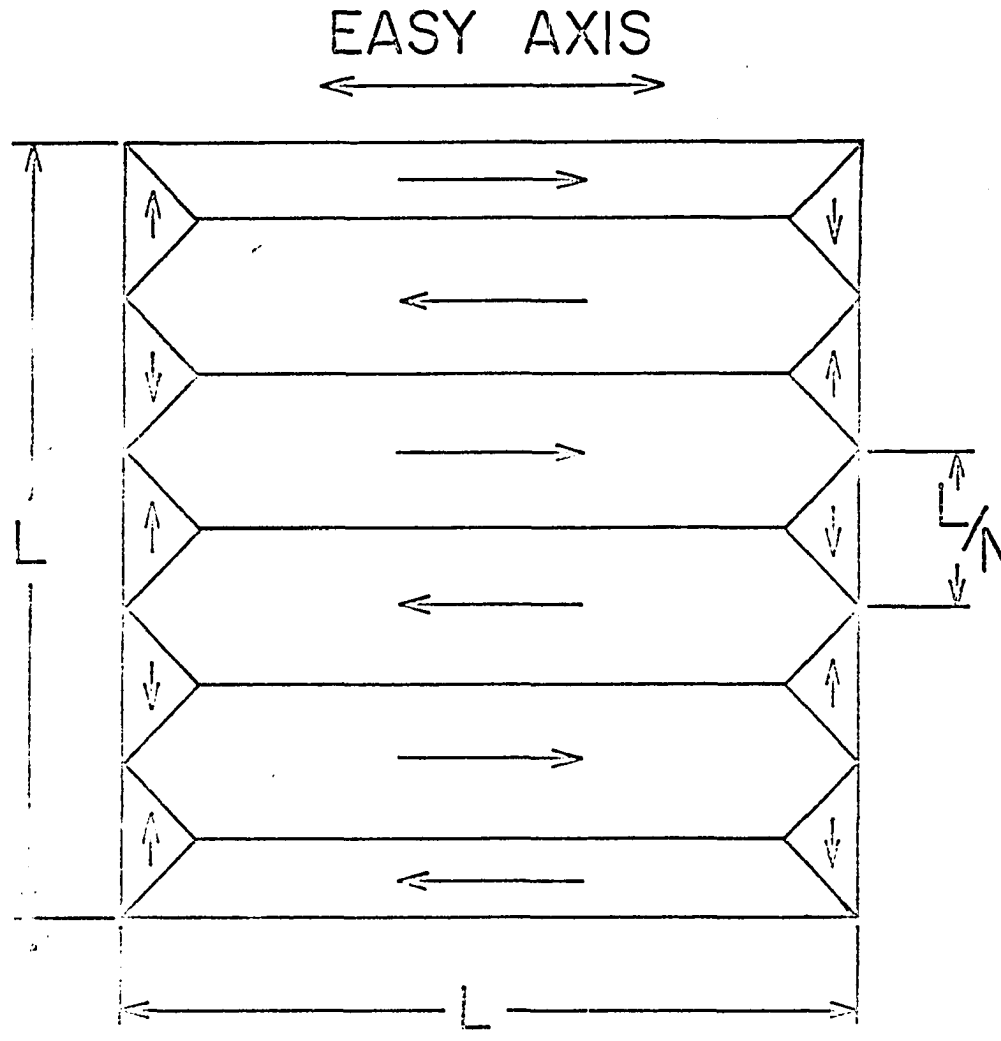
EASY AXIS
L
L/N
L

and

$$N = \sqrt{\frac{KL}{2\upsilon_{wall}}} \quad .$$

Using typical values (1) of $\upsilon_{wall} \simeq 5$ ergs cm^2 and $K \simeq 1000$ ergs/cm^3, one finds $N \simeq \sqrt{100\ L}$, where L is in cm. Note that the number of strips decreases as L decreases, and as a rough approximation, N is smaller than 10 as L decreases below 1 cm.